

SYNTHESIS, STRUCTURAL, OPTICAL AND MAGNETIC PROPERTIES OF Ni CO-DOPED ZnO:Al NANOPARTICLES

J. EL GHOUL^{a,b,*}, G. A. KHOUQEER^a

^a*Department of Physics, College of Sciences, Imam Mohammad Ibn Saud University (IMSIU), Riyadh 11623, Saudi Arabia*

^b*Laboratory of Physics of Materials and Nanomaterials Applied at Environment (LaPhyMNE), Gabes University, Faculty of Sciences in Gabes, 6072, Tunisia*

In this work, we investigate structural, optical and magnetic properties of Zn_{0.89}Ni_{0.1}Al_{0.01}O nanoparticles synthesized by sol-gel. In our protocol, the water has been slowly released following an esterification reaction, then, this solution was dried under supercritical conditions of ethyl alcohol and heat treatment in air at 500°C for 2 hours. The structural and morphological properties showed that the obtained samples have a wurtzite structure with a crystallite size around 25 nm and a secondary phase has been detected, attributed to NiO phase. UV-Vis spectroscopy shows that a band gap of 3.368 eV was obtained, a value close to that of bulk ZnO. Magnetic measurements at 10K and 300K showed a superparamagnetic.

(Received July 12, 2020; Accepted September 27, 2020)

Keywords: ZnO, Semiconductors, Sol-gel, Structural properties, Magnetic properties

1. Introduction

Zinc oxide (ZnO) nanoparticles (NPs) with unique physical and chemical properties have attracted significant interest in industrial application, such as light-emitting diode, photocatalysis, sensors, and solar cell [1-3]. In particular, ZnO doped with various elements have been predicted in theory as well as a practice to be effective diluted magnetic semiconductors (DMS) with high Curie temperatures, which make it an important role in magneto-electronic and magneto-optical devices. There are three typical dopants to obtain room temperature ferromagnetism (FM) ZnO, including transition metal (TM, e.g., Co, Fe, Ni) [4-6], rare earth (RE, e.g., Gd, Eu, Tb) [7-9], as well as nonmagnetic element (e.g., Li, Al, C) [10,11]. Their FM properties mainly arise from intrinsic defects related to vacancies or interstitials [10]. Some researchers also attribute the origin of magnetism of TM- or RE-doped ZnO to the presence of dopant-related secondary phases, such as metallic clusters or metallic oxide [8, 9]. In addition, Yi et al. [12] proposed that doping appropriate elements into ZnO could stabilize cation vacancies and form holes to improve the FM properties.

ZnO NPs co-doped with Al and transition metals are important function materials for optoelectronic and magnetoelectronic applications. The transition metals generally used are Co and Mn [13-17]. Recently, we have prepared the Ni and Al co-doped ZnO films on glass substrates by direct current (DC) magnetron co-sputtering [18,19]. The films had the room temperature ferromagnetism, dependent on the deposition temperature and the Ni content. Furthermore, the film, which exhibited the better ferromagnetic behavior, had the relatively high resistivity. It is a significant work to prepare the Ni and Al codoped ZnO nanoparticles having better electrical and ferromagnetic behaviors for their potential applications.

Recently, we have prepared Al and Ni co-doped ZnO films using direct current (DC) magnetron co-sputtering and have studied their structural, electrical, optical and magnetic properties [20-22]. The Ni content in the films ranged from 4 at% to 11 at%. It was found that for the Al and Ni co-doped ZnO film the ferromagnetic behavior was enhanced by increasing Ni

* Corresponding author: ghoultn@yahoo.fr

content. However, the optical transmittance in the visible wavelength range decreased and the resistivity increased with increasing Ni content. It is desirable to prepare Al and Ni co-doped ZnO films with high saturation magnetization, low resistivity and high transparency. While it was reported that annealing could improve the structural and physical properties of TM doped ZnO films [23–27], it has not been reported, to our best knowledge, how vacuum magnetic annealing does to the films.

In the present work, $\text{Zn}_{0.89}\text{Ni}_{0.1}\text{Al}_{0.01}\text{O}$ is prepared by sol-gel for different applications. The structure of the nanoparticles is studied using X-ray diffraction (XRD), scanning electron microscopy (SEM) and transmission electron microscopy (TEM). The optical and magnetic properties are measured by UV-Vis-IR spectrophotometer and a vibrating sample magnetometer (VSM), respectively.

2. Experimental details

2.1. Sample preparation

Ni and Al codoped ZnO aerogel nanopowders were synthesized by dissolving 2 g of zinc acetate dihydrate ($\text{Zn}(\text{CH}_3\text{COO})_2 \cdot 2\text{H}_2\text{O}$) in 14 mL of methanol. After 30 min magnetic stirring at room temperature, adequate quantity of nickel chloride hexahydrate ($\text{NiCl}_2 \cdot 6\text{H}_2\text{O}$) and aluminum nitrate-9-hydrate [$\text{Al}(\text{NO}_3)_3 \cdot 9\text{H}_2\text{O}$] were added. After 15 min of magnetic stirring, the solution was placed in an autoclave and dried under supercritical conditions in ethyl alcohol (EtOH). The obtained powders were divided into two parts. The first one was analyzed as-synthesized and the second one was annealed at different temperatures in air for 2 h.

2.2. Characterization techniques

The structural properties of nanopowders were performed using Bruker D8 Discover diffractometer (θ - 2θ) equipped with Cu-K α radiation ($\lambda=1.5406 \text{ \AA}$). We used a JEM-200CX transmission electron microscope (TEM) to study the morphology of our samples. The TEM samples were prepared by mixing a very weak mass of nanoparticles in ethyl alcohol in an ultrasonic bath towards 15 minutes, and then we dropped one or two drops of the obtained solution on the TEM grid. The absorbance measurement was performed by a UV-Vis-IR spectrophotometer (Shimadzu UV-3101 PC) using an integrating sphere intended for these types of samples in the wavelength range from 200 to 1800 nm. Magnetic spectra have been realized in a Quantum Design MPMS-5S SQUID magnetometer.

3. Results and discussion

3.1. Structural analysis

Fig. 1 shows typical XRD spectra of the three prepared samples. The patterns reveal that the structure is a polycrystalline wurtzite structure of ZnO with hexagonal phase (ICDD file No. 36-1451) [28]. We should note the appearance of an additional weak peak at around 37° which is attributed either to the production of phase separation [29], or to the presence of secondary phases attributed to a NiO [30]. In contrast, no diffraction peak related to Al was detected, which indicates the total doping Al within ZnO host lattice.

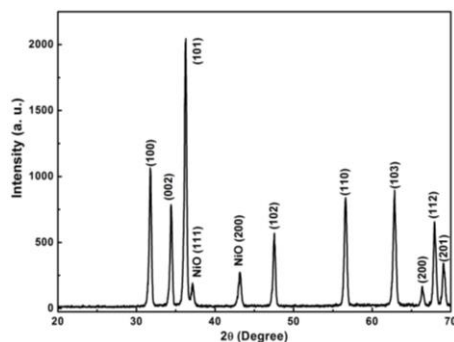


Fig. 1. X-ray diffraction spectrum of $Zn_{0.89}Ni_{0.1}Al_{0.01}O$ nanoparticles.

Due to the small size of the crystallites in the nanoparticles, the diffraction lines are broadened and are further found to depend on the Miller indices of the corresponding sets of crystal planes. The average grain size can be calculated using the Debye-Scherrer equation [31]:

$$G = 0.9\lambda / B \cos \theta_B \quad (1)$$

where λ is the X-ray wavelength (1.5418 Å), θ_B is the maximum of the Bragg diffraction peak and B is the linewidth at half maximum. After a correction for the instrumental broadening, an average value of the crystallites size is found to be 28 nm. From the symmetric peaks, we find that the lattice parameter c ($c = 5.2112$ Å) is close to the value of conventional nanosized crystallites {ICDD file No. 67848–1993 (5.2151 Å) and 67454–1989 (5.2071 Å)}.

3.2. Morphological analysis

The morphology of the Ni-doped ZnO investigated using SEM is shown in Fig. 2. A glance at the SEM image of the sample shows a group of dark and bright regions. This SEM micrograph reveals the presence of the cluster formations surrounded by the pores. It is clearly observed that the cluster comprises of some hexagonale shaped particles. The EDAX analysis of ZnO:Ni nanoparticles is carried out to establish purity of the samples and confirm presence of Ni and Al in them. It is noticed from Fig. 3 that the samples prepared contain only Zn, Ni, Al and O. Thus the nanocrystallites are found to contain no spurious contamination. The ratio of the atomic percentage of the elements present in the sample complies with the quantity taken for their preparation.

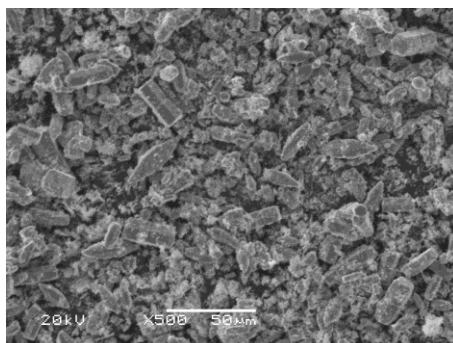


Fig. 2. SEM image of $Zn_{0.89}Ni_{0.1}Al_{0.01}O$ nanoparticles.

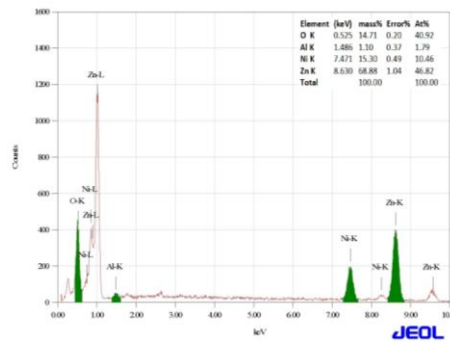


Fig. 3. EDAX elemental mapping of $Zn_{0.89}Ni_{0.1}Al_{0.01}O$ nanoparticles.

Fig. 4 shows the TEM image of our sample. The observed morphology reveals the presence of an almost spherical shape with diameters ranging from 25 to 40 nm. This indicates that the crystallite size is nanometric and conforms to the results of the XRD.

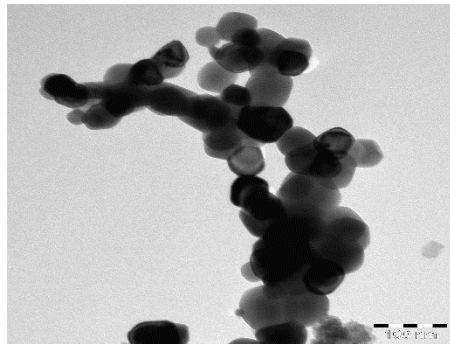


Fig. 4. TEM image of $Zn_{0.89}Ni_{0.1}Al_{0.01}O$ nanoparticles.

3.3. Optical properties

The spectra shown in Fig. 5 reveal the absorbance of the three samples showing a high absorption in the spectral range between 300 and 400 nm and intense transmittance in the visible range. This is known as one of the characteristics of nano-ZnO.

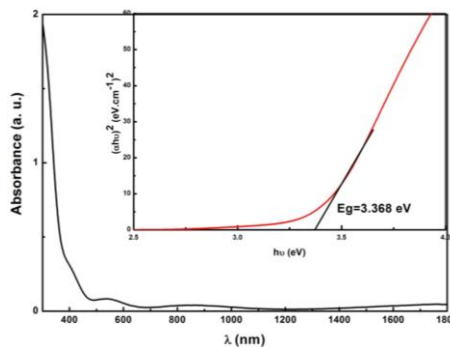


Fig. 5. Absorbance spectra at room temperature. In-set the plot of $(ahv)^2$ as a function of $h\nu$.

The absorption coefficient α is related to the optical energy band gap E_g for high photon energies as [32]:

$$\alpha(h\nu) = C(h\nu - E_g)^{\frac{1}{2}} \quad (1)$$

where C is a direct transition constant, and $h\nu$ present the energy intensity of incident photon. The plot of $(\alpha h\nu)^2$ vs. $(h\nu)$ reveals a linear variation, indicating that the semiconductor is direct transition type. The plot of $(\alpha h\nu)^2$ versus photon energy, as shown inset Fig. 5, present a direct band gap (E_g) value to be 3.368 eV.

3.4. Magnetic properties

In addition to its known major diamagnetic property, ZnO has a paramagnetic and weak ferromagnetic component (RT-FM) at room temperature [33, 34]. Almost all authors have attributed this RT-FM either to the creation of defects in the structure such as vacancies or small size of the grains [35,36]. Recently, the improvement of ferromagnetic characteristic by doping with a non-magnetic material such as Al-doped ZnO has been noticed [37]. The authors attached this characteristic (FM) to the formation of oxygen vacancies and Zn interstitials according to the doping, which can be demonstrated using the bound magnetic polaron model. In addition, this phenomenon may be due to grain boundaries, as has been discussed by Straumal et al. [38].

Fig. 6 shows magnetization hysteresis (M–H) curves of our sample at 300 K and 10 K. The magnetization has been observed not to saturate and do not show any significant hysteresis, coercivity, and retentivity and thus it clearly shows the feature of superantiferromagnetic/superparamagnetic behaviour. It has been reported previously that NiO is an antiferromagnetic material with Neel temperature of 520 K, while at room temperature it is super paramagnetic [44]. XRD study of our sample confirms the existence of secondary phase NiO, suggesting this hypothesis.

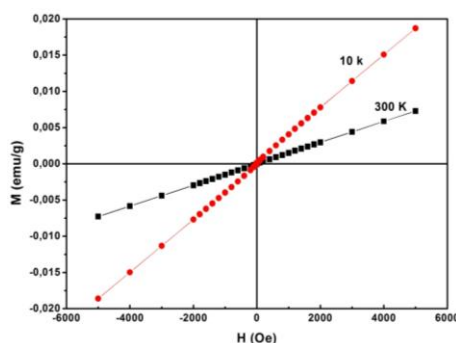


Fig. 6. Magnetization vs. magnetic field (M-H) of the $Zn_{0.89}Ni_{0.1}Al_{0.01}O$ nanoparticles at 300 K and 10 K.

4. Conclusion

Nickel and aluminium co-doped ZnO nanoparticles were synthesized by sol-gel method. The structural and morphological indicated the appearance of wurtzite structure of ZnO with hexagonal phase. In addition, the crystallite size decreases with increasing Gd concentration, while the strain enhanced. XRD revealed the nanometric scale and the presence of secondary phases related to the Ni complex. The obtained value of band gap is close to that of bulk ZnO. In addition, the samples show superparamagnetic behaviours attributed to NiO phase.

Acknowledgments

The authors extend their appreciation to the Deanship of Academic Research at Imam Mohamed Ibn Saud Islamic University (IMSIU), Riyadh, Kingdom of Saudi Arabia, for funding the work through research project Number 18-11-12-015, 1441H.

References

- [1] H. Zhou, G. Fang, L. Yuan, C. Wang, X. Yang, H. Huang, C. Zhou, X. Zhao, *Appl. Phys. Lett.* **94**, 013503 (2009).
- [2] E. Alkuam, M. Mohammed, T. P. Chen, *Sol Energy* **150**, 317 (2017).
- [3] J. El Ghoul, C. Barthou, L. El Mir, *Physica E* **44**, 1910 (2012).
- [4] T. A. Abdel-Baset, Y. W. Fang, B. Anis, C. G. Duan, M. Abdel-Hafiez, *Nanoscale Res. Lett.* **11**, 115 (2016).
- [5] M. Shatnawi, A. M. Alsmadi, I. Bsoul, B. Salameh, G. A. Alnawashi, F. Al-Dweri, F. E. Akkad, *J. Alloy. Compd.* **655**, 244 (2016).
- [6] J. Jadhav, S. Biswas, *J. Alloy. Compd.* **664**, 71 (2016).
- [7] G. S. Lotey, J. Singh, N. K. Verma, *J. Mater. Sci. Elec.* **24**, 3611 (2013).
- [8] G. J. Huang, J. B. Wang, X. L. Zhong, G. C. Zhou, H. L. Yan, *J. Mater. Sci.* **42**, 6464 (2007).
- [9] J. El Ghoul, C. Barthou, L. El Mir, *J. Superlattices Microstruct.* **51** (2012) 942.
- [10] D. Q. Alo, J. Zhang, G. J. Yang, J. L. Zhang, Z. H. Shi, J. Qi, Z. H. Zhang, D. S. Xue, *J. Phys. Chem. C* **114**, 13477 (2010).
- [11] S. Chawla, K. Jayanthi, R. K. Kotnala, *Phys Rev B* **79**, 125204 (2009).
- [12] J. B. Yi, C. C. Lim, G. Z. Xing, H. M. Fan, L. H. Van, S. L. Huang, K. S. Yang, X. L. Huang, X. B. Qin, B. Y. Wang, T. Wu, L. Wang, H. T. Zhang, X. Y. Gao, T. Liu, A. T. S. Wee, Y. P. Feng, J. Ding, *Phys. Rev. Lett.* **104**, 137201 (2010).
- [13] M. Venkatesan, P. Stamenov, L. S. Dorneles, R. D. Gunning, B. Bernoux, J. M. D. Coey, *Appl. Phys. Lett.* **90**, 242508 (2007).
- [14] A. J. Behan, A. Mokhtari, H. J. Blythe, D. Score, X. H. Xu, J. R. Neal, A. M. Fox, D. A. Gehring, *Phys. Rev. Lett.* **100**, 047206 (2008).
- [15] K. Samanta, P. Bhattacharya, J. G. S. Duque, W. Iwamoto, C. Rettori, P. G. Pagliuso, R. S. Katiyar, *Solid State Commun.* **147**, 305 (2008).
- [16] M. Sharma, R. M. Mehra, *Appl. Surf. Sci.* **255**, 2527 (2008).
- [17] S. K. Neogi, R. Ghosh, G. K. Paul, S. K. Bera, S. Bandyopadhyay, *J. Alloys Compd.* **487**, 269 (2009).
- [18] T. F. Li, H. Qiu, P. Wu, M. W. Wang, R. X. Ma, *Thin Solid Films* **515**, 3905 (2007).
- [19] M. P. Yu, H. Qiu, X. B. Chen, H. X. Liu, M. W. Wang, *Physica B* **404**, 1829 (2009).
- [20] T. F. Li, H. Qiu, P. Wu, M. W. Wang, R. X. Ma, *Thin Solid Films* **515**, 3905 (2007).
- [21] M. P. Yu, H. Qiu, X. B. Chen, H. X. Liu, M. W. Wang, *Physica B* **404**, 1829 (2009).
- [22] M. P. Yu, H. Qiu, X. B. Chen, H. X. Liu, *Mater. Chem. Phys.* **120**, 571 (2010).
- [23] Y. M. Cho, W. K. Choo, H. Kim, D. Kim, Y. Ihm, *Appl. Phys. Lett.* **80**, 3358 (2002).
- [24] H. S. Hsu, J. C. A. Huang, Y. H. Huang, Y. F. Liao, M. Z. Lin, C. H. Lee, J. F. Lee, S. F. Chen, L. Y. Lai, C. P. Liu, *Appl. Phys. Lett.* **88**, 242507 (2006).
- [25] N. Khare, M. J. Kappers, M. Wei, M. G. Blamire, J. L. MacManus-Driscoll, *Adv. Mater.* **18**, 1449 (2006).
- [26] B. Huang, D. L. Zhu, X. C. Ma, *Appl. Surf. Sci.* **253**, 6892 (2007).
- [27] E. Liu, P. Xiao, J. S. Chen, B. C. Lim, L. Li, *Curr. Appl. Phys.* **8**, 408 (2008).
- [28] Powder Diffraction File, Joint Committee for Powder Diffraction Studies (JCPDS) File No. 36-1451.
- [29] Mohammed M. Obeid, Shaker J. Edrees, Majid M. Shukur, *Superlattices and Microstructures*, **122**, 124 (2018).
- [30] N. Srivastava, P. C. Srivastava, *Bull. Mater. Sci.* **33**, 653 (2010).
- [31] J. El Ghoul, N. Bouguila, S. A. Gómez-Lopera, L. El Mir, *Superlattices and Microstructures*

- 64**, 451 (2013).
- [32] J. El Ghoul, L. El Mir, *J Mater Sci: Mater Electron.* **28**, 9066 (2017).
- [33] S. Zhou, Q. Xu, K. Potzger, G. Talut, R. Greetzschel, J. Fassbender, M. Vinnichenko, J. Grenzer, M. Helm, H. Hochmuth, M. Lorenz, M. Grundmann, H. Schmidt, *Appl. Phys. Lett.* **93**, 232507 (2008).
- [34] J. El Ghoul, M. Kraini, O.M. Lemine, L El Mir. *J Mater Sci: Mater Electron.* **26**, 2614 (2015).
- [35] Z. Li, W. Zhong, X. Li, H. Zeng, G. Wang, W. Wang, Z. Yang, Y. Zhang, *J. Mater. Chem. C* **2013**, 6807 (2013).
- [36] J. El Ghoul, F.F. Al-Harbi, *Solid State Communications* **314-315**, 113916 (2020).
- [37] Teng-Tsai Lin, San-Lin Young, Chung-Yuan Kung, Hone-Zern Chen, Ming-Cheng Kao, Neng-Fu Shih, Jen-Bin Shi, Jia-He You, *Jpn. J. Appl. Phys.* **52**, 11NJ12 (2013).
- [38] Boris B. Straumal, Andrei A. Mazilkin, Svetlana G. Protasova, Petr B. Straumal, Ata A. Myatiev, Gisela Schütz, Eberhard J. Goering, Thomas Tietze, Brigitte Baretzky, *Phil. Mag.* **93**, 1371 (2013).
- [39] D. Guruvammal, S. Selvaraj, S. Meenakshi Sundar, *Journal of Alloys and Compounds* **682**, 850 (2016).